Evaluation of Cervical Lymph Nodes in Head and Neck Cancer With CT and MRI: Tips, Traps, and a Systematic Approach

Jenny K. Hoang[1,2]
Jyotsna Vanka[1]
Benjamin J. Ludwig[1]
Christine M. Glastonbury[3]

OBJECTIVE. In this article, we present a 4-step approach to evaluating lymph nodes in the setting of head and neck squamous cell and thyroid carcinoma and highlight important tips and traps.

CONCLUSION. The presence and extent of nodal metastases in head and neck cancer has a great impact on treatment and prognosis. Pretreatment CT and MRI of the neck are commonly performed to evaluate for nodal metastases.

Keywords: cervical lymph nodes, CT, head and neck, lymphadenopathy, squamous cell carcinoma

DOI:10.2214/AJR.12.8960

Received April 5, 2012; accepted after revision June 10, 2012.

J. Hoang is a GE Research Academic Fellow.
C. M. Glastonbury is a consultant to and investor in Amirsys.

[1]Department of Radiology, Duke University Medical Center, Box 3808, Erwin Rd, Durham NC, 27710. Address correspondence to J. K. Hoang (jennykh@gmail.com).

[2]Department of Radiation Oncology, Duke University Medical Center, Durham, NC.

[3]Department of Radiology and Biomedical Imaging, Otolaryngology-Head and Neck Surgery, and Radiation Oncology, University of California, San Francisco, San Francisco CA.

CME/SAM
This article is available for CME/SAM credit.

WEB
This is a Web exclusive article.

AJR 2013; 200:W17–W25

0361–803X/13/2001–W17

Nodal metastases have a great impact on treatment and prognosis in head and neck cancer. A solitary lymph node metastasis from head and neck squamous cell carcinoma has a 5-year survival rate of 50% and an additional contralateral nodal metastasis reduces the survival to 33% [1]. Detection of nodal metastasis by imaging is more accurate than clinical examination; thus, it has become routine to perform CT or MRI as workup for head and neck cancer.

The imaging assessment of nodal disease can be challenging for the radiologist because there are multiple sites to review and differing opinions about criteria for abnormal nodes. The ability to accurately detect nodal metastases is improved with knowledge of the criteria for abnormal nodes, the nodal drainage patterns, and common imaging pitfalls. In this article, we introduce these basic concepts through a systematic 4-step approach for evaluation of metastatic cervical lymph nodes on cross-sectional neck imaging.

Imaging Approach

We recommend a systematic approach to evaluating and reporting cervical lymph nodes for head and neck squamous cell carcinoma (HNSCC) and thyroid carcinoma that involves four steps: systematically search for abnormal nodes, particularly in expected drainage sites; describe location and review check locations (Fig. 1); report features important for staging; and evaluate features important for management.

Step 1: Criteria for Abnormal Nodes

Abnormal nodes are categorized on the basis of size, morphology, shape, margins, and distribution.

Size—Evaluating abnormal nodes by size is confusing because there are multiple size criteria reported in the literature for cervical lymph nodes, ranging from 7 mm to 3 cm [2, 3]. Additionally, the criteria can vary for different nodal sites and patient age. Submandibular and jugulodigastric nodes are more likely to be affected by benign hyperplasia than other nodal groups, and lymph nodes can normally be larger and more numerous in younger patients.

The method of measuring lymph nodes is another source of variation. Nodes can be measured in either the short or long axis, and they can be measured only on axial images or include diameters in the craniocaudal dimension on reformatted images [2, 3]. RECIST (Response Evaluation Criteria In Solid Tumors) 1.1 measures lymph nodes in the short axis on axial images. Nodes ≥ 15 mm are pathologically enlarged and measurable, and lymph nodes measuring 10–15 mm in short axis are reportable as pathologic nontarget sites [4].

In clinical practice, size is not a reliable marker of malignancy. Small nodes can harbor small metastases that do not expand the node, and, conversely, benign nodes can commonly be enlarged due to hyperplasia or inflammation. The radiologist's choice of size cutoff simply changes sensitivity and specificity for detection of nodal metastases. Curtin et al. [3] evaluated the sensitivity and specificity of dif-

ferent size criteria for HNSCC metastatic disease and found that a 1-cm size cutoff in the largest axial diameter achieved 88% sensitivity and 39% specificity, whereas a 1.5-cm cutoff resulted in 56% sensitivity and 84% specificity.

For head and neck cancer staging, it is generally more important to have higher sensitivity. Although we use 1-cm short-axis cutoff on axial images, we acknowledge this could still result in a high false-negative rate.

Tip—Nodes less than 1 cm in size can still be malignant and should be carefully evaluated for other abnormal features, particularly if in expected drainage sites of the primary tumor (Fig. 2).

Tip—If these nodes are still not definitively malignant by CT or MRI criteria, they should be evaluated further if there will be a change in patient management, such as altering neck dissection plans or changing radiation field or dose. Ultrasound is an excellent second-line tool for evaluating these suspicious nodes and can also guide fine-needle aspiration to obtain cytology (Fig. 3).

Morphology—Metastatic disease can replace normal fatty hila with findings of necrosis, cystic change, calcification, or hyperenhancement.

Nodal necrosis in the presence of a head and neck cancer primary tumor is the most valuable sign of metastatic involvement, with specificity between 95% and 100% [5]. Necrotic nodes have focal CT hypoattenuation or T2 MRI hyperintensity with irregular peripheral solid enhancement (Fig. 4). The center pathologically represents necrosis due to obstruction of lymphatic flow but can also contain tumor cells, fibrous tissue, and edematous fluid. Necrotic nodes are most commonly from HNSCC but may uncommonly occur with lymphoma.

Trap—Partial volume artifact of normal fatty hila may mimic nodal necrosis (Fig. 3).

Tip—In the setting of head and neck cancer, necrotic or cystic change, even in small nodes, is a specific marker of malignancy.

Cystic nodes have components of the lymph node replaced by fluid density or signal and have a thin wall (Fig. 5). Primary sites to consider with cystic morphology are papillary thyroid cancer and oropharyngeal HNSCC. Thyroid cystic metastases may have hyperin-

TABLE 1: Site Classification for Lymph Nodes From American Head and Neck Society and American Academy of Otolaryngology-Head and Neck Surgery

Level	Anatomic Name	Key Borders and Landmarks	Primary Drainage Site
I	IA = submental; IB = submandibular	Hyoid bone	Anterior oral cavity, lip, sinonasal
		Posterior margin of submandibular gland	
		IA or IB—anterior belly of digastric muscle	
II	Anterior cervical or upper jugular	Inferior margin of hyoid	Oropharynx, posterior oral cavity, supraglottic larynx, parotid gland
		Posterior margin of submandibular gland	
		Posterior margin of sternocleidomastoid	
		IIA or IIB—posterior margin of internal jugular vein	
III	Middle jugular	Inferior margin of hyoid	Glottic, subglottic, and hypopharyngeal regions
		Inferior margin of cricoid	
IV	Lower jugular	Inferior margin of cricoid	Subglottic, thyroid, and cervical esophagus
		Clavicle	
V	Posterior compartment or spinal accessory	Posterior border of sternocleidomastoid	Nasopharynx; skin carcinomas of the neck or occipital scalp
		Clavicle	
		VA or VB—inferior margin of cricoid	
VI	Visceral or central compartment	Medial margins of carotid arteries	Subglottic; thyroid and cervical esophagus
		Inferior margin of hyoid	
		Superior aspect of manubrium	
VII	Superior mediastinal	Superior aspect of manubrium	Subglottic; thyroid and cervical esophagus
		Innominate vein	
	Retropharyngeal	Medial margin of internal carotid arteries to the level of hyoid	Nasopharynx, oral cavity, sinonasal, thyroid, and pharyngeal and laryngeal tumors with posterior wall involvement
	Parotid	Within parotid gland	Skin of scalp, orbit, nasopharynx
	Supraclavicular fossa[a]	On axial images at or below the clavicle, lateral to the medial edge of the common carotid artery, and medial to clavicle; includes some level IV and V nodes	Any head and neck cancer and cancers of the thorax and abdomen, including lung, breast, esophageal, gastric, pancreatic, gynecologic, and prostate cancers

Note—See Figure 1 for description of levels I–V.

[a]The supraclavicular fossa is better defined on palpation as the Ho triangle, a triangular plane defined by three points: upper sternal end of the clavicle, upper lateral end of the clavicle, and point at which the posterior portion of the neck meets the shoulder. On imaging, the clavicle can be elevated, leading to erroneously high classification of the supraclavicular fossa node.

tense signal on T1-weighted MRI due to thyroid protein or blood products (Fig. 6). Oropharyngeal HNSCC nodal metastases can be purely cystic or necrotic and if seen in the absence of traditional risk factors, such as smoking and alcohol, the radiologist should consider human papillomavirus (HPV)-associated HNSCC [6, 7] (Fig. 4).

Trap—Do not dismiss cystic neck lesions as congenital cysts in adults. HPV-associated HNSCC and thyroid malignancy may have purely cystic metastases, and both can occur in young adults (Fig. 4).

Trap: Cystic or necrotic nodes can be large with a small or occult primary tumor. In particular, small tumors of the base of tongue and tonsil are frequently not symptomatic and can be overlooked on imaging (Fig. 4).

Calcified lymph nodes are most commonly found with thyroid carcinoma due to the presence of psammomatous calcifications with papillary and medullary carcinoma (Fig. 5). The calcifications in papillary carcinoma may have a speckled appearance. Other causes of nodal calcification are mucinous adenocarcinoma; treated lymphoma; treated or untreated HNSCC; and, less commonly, tuberculosis [8].

Trap—Although mediastinal nodal calcifications are usually a marker of benign disease, cervical nodal calcifications are more frequently seen with malignancy.

Shape and margins—A normal lymph node has a reniform shape and smooth well-defined margins. Metastatic disease can change the shape of the node by infiltrating nodal tissue and expanding the nodal capsule. Thus, rounded rather than oval nodes are suspicious. As disease progresses, the capsule no longer contains the node; ill-defined irregular margins in a lymph node are a sign of malignancy and may represent extracapsular spread of tumor (Fig. 7).

Trap—A recent lymph node biopsy or radiation may result in inflammation and ill-defined margins that can mimic extracapsular spread.

Distribution—Asymmetrically prominent nodes or three or more contiguous and confluent lymph nodes along the drainage chain of a primary tumor should be viewed with a high degree of suspicion [9].

Step 2: Site Classification and Check Sites

Site classification—When an abnormal node is detected, it should be classified to a site on the basis of the system devised by American Head and Neck Society and American Academy of Otolaryngology-Head and Neck Surgery [10, 11] (Fig. 1). This system uses Roman numerals to define levels. Compared with anatomic names, this system is a more reproducible method of describing lymph nodes for targeted therapy with surgical resection or radiation therapy.

Classifying the nodal site and considering the location also improve diagnostic accuracy for borderline abnormal nodes. Each nodal site corresponds with first-order drainage locations for specific ipsilateral primary tumors (Table 1). Familiarity with drainage patterns is important; it guides radiologists to carefully examine the likely sites of metastasis (Figs. 7–9), and improves the negative predictive value for nodes not likely to be draining the tumor. Additionally, for an unknown primary tumor, familiarity with nodal drainage allows greater scrutiny of potential primary sites. Carcinoma with an unknown primary tumor represents less than 5% of all head and neck cancers [12], but detection of the primary mucosal tumor may then direct the surgeon's endoscopic examination and prevent a more invasive diagnostic workup and more extensive radiation therapy [13].

Tip—Midline tumors, nasopharyngeal carcinoma (NPC), and epiglottic and oral cavity tumors frequently drain bilaterally (Fig. 2).

Tip—If a lower level neck node is abnormal, a higher level should be carefully evaluated.

TABLE 2: Nodal Staging in Oropharyngeal, Hypopharyngeal, Laryngeal, Oral Cavity and Sinonasal Carcinoma

N Stage	Criteria	Key Feature That Upstages From Lower Nodal Stage
N0	No regional lymph node metastasis	
N1	Single, ipsilateral lymph node < 3 cm in greatest dimension	
N2a	Single ipsilateral lymph node, 3–6 cm in greatest dimension	Size
N2b	Multiple ipsilateral lymph nodes, ≤ 6 cm in greatest dimension	Number
N2c	Bilateral or contralateral lymph nodes ≤ 6 cm in greatest dimension	Laterality
N3	Lymph node(s) > 6 cm in greatest dimension	Size

TABLE 3: Nodal Staging in Nasopharyngeal Carcinoma

N Stage	Criteria	Key Feature That Upstages From Lower Nodal Stage
N0	No regional lymph node metastasis	
N1	Unilateral lymph node(s) ≤ 6 cm in greatest dimension and above supraclavicular fossa[a]	
	Unilateral or bilateral retropharyngeal node(s) measuring ≤ 6 cm in greatest dimension	
N2	Bilateral lymph node(s) ≤ 6 cm in greatest dimension and above supraclavicular fossa	Laterality
N3a	Unilateral or bilateral lymph node(s) measuring > 6 cm in maximal dimension	Size
N3b	Lymph node(s) extending into supraclavicular fossa	Special site: supraclavicular fossa

[a]The supraclavicular fossa is better defined on palpation as the Ho triangle, a triangular plane defined by three points: upper sternal end of the clavicle, upper lateral end of the clavicle, and point at which the posterior portion of the neck meets the shoulder. On imaging, the clavicle can be elevated, leading to erroneously high classification of the supraclavicular fossa node.

TABLE 4: Nodal Staging in Differentiated Thyroid Carcinoma

N Stage	Criteria	Key Feature That Upstages From Lower Nodal Stage
N0	No regional nodal metastasis	
N1a	Level VI (pretracheal, paratracheal, and prelaryngeal nodes)	
N1b	Unilateral, bilateral, or contralateral nodes (levels I–V)	Special site: outside level VI
	Any retropharyngeal or superior mediastinal nodes (level VII)	

Check sites—The check locations are sites where metastases can be missed. Retropharyngeal nodes and parotid nodes are not classified in levels I–VII and can be forgotten (Figs. 8 and 9). These two groups may not be palpable on clinical examination; therefore, the role of the radiologist is important. The other nodes that should be reviewed carefully are the superficial nodes when a skin cancer is the primary tumor (Figs. 7 and 10).

Trap—Retropharyngeal and parotid nodes may be overlooked when they drain primary tumors that are remote in location. Thyroid and nasopharyngeal cancers can drain to the retropharyngeal nodes and NPC can drain to the parotid (Figs. 8 and 9 and Table 1).

Trap—Skin cancer metastasizes to level V and superficial nodes, such as parotid, posterior auricular, facial, and occipital nodes (Figs. 7 and 10).

Tip—The Virchow node is a left supraclavicular lymph node near the junction of the thoracic duct and the left subclavian vein where the lymph from much of the body drains into the systemic circulation. When this is an isolated finding on neck CT or MRI, the main differential diagnoses are thyroid cancer and thoracic and abdominal malignancy (Table 1).

Step 3: Features Important for Staging

The American Joint Committee on Cancer (AJCC) nodal (N) staging system for HNSCC is the same for larynx, hypopharynx, oropharynx, oral cavity, and sinonasal tumors [14] (Table 2). The final N stage is a combination of clinical examination, imaging, and pathology. The radiologist's role is to describe three characteristics pertinent to the N staging: size, single versus multiple nodes, and side of nodes. Each of these three characteristics can result in a higher N stage.

Tip—Look for small metastases that will upstage the N stage. If there is a single node, look for another node. If there is ipsilateral disease, evaluate contralateral nodes (Fig. 2).

Tip—If there are no clearly abnormal nodes, carefully reexamine the expected first-order draining nodes before reporting N0 disease.

NPC and thyroid carcinoma have entirely different AJCC nodal staging systems from most head and neck cancers, reflecting the relative better prognosis despite nodal disease (Tables 3 and 4). These staging systems emphasize special sites, such as supraclavicular and retropharyngeal nodes.

Tip—The supraclavicular nodes in NPC and retropharyngeal nodes in thyroid carcinoma are lower-level nodes and represent more advanced nodal disease. The presence of these nodal groups should lead to a careful search of systemic metastases, most commonly in the lung.

Step 4: Features Important for Management

Local invasion of a lymph node first occurs beyond the nodal capsule and then into adjacent structures. The characteristics of extracapsular spread are poor prognostic indicators and associated with reduced survival (further 50%) [15] but do not currently alter the AJCC TNM stage. It has been recommended that extracapsular spread+ or extracapsular spread− be added as descriptors until further data determine whether extracapsular spread+ alters N staging [14].

Imaging findings of extracapsular spread are irregular margins, fat stranding, and loss of fat planes with adjacent structures. Extracapsular spread is more likely in larger nodes. It is present in the majority of squamous cell carcinoma nodes > 3 cm, but 25% of nodes measuring < 1 cm may still have pathologic extracapsular spread [16] (Fig. 7).

Trap—Biopsied or infected lymph nodes may mimic extracapsular spread.

Nodal metastases can invade adjacent muscle, bone, neural, and vascular structures (Figs. 10 and 11). Arterial invasion affects surgical options and leads to devastating vascular complications, such as occlusion, pseudoaneurysm, and carotid blowout. The most sensitive sign of arterial invasion is loss of fascial planes, and the most specific sign is narrowing or irregularity of the artery [17]. Another important sign of arterial invasion is circumferential arterial encasement by > 180–270°, which is associated with increased likelihood of adventitial invasion and portends a grave prognosis [17–19] (Fig. 11).

Advanced Imaging Techniques for Nodal Metastases

Other techniques for evaluating cervical nodes are ^{18}F-FDG PET, diffusion-weighted MRI (DWI), perfusion imaging with dynamic contrast-enhanced MRI (DCE-MRI), and CT perfusion [20]. FDG PET is most commonly performed in clinical practice. In a meta-analysis that compared FDG PET with CT, MRI, or sonography, FDG PET increased sensitivity for nodal metastases from 79% to 85% and increased specificity from 80% to 86% [21] (Fig. 2). Pretreatment FDG PET for N-staging is particularly useful in several clinical scenarios: high tumor (T) stage with less nodal disease than expected, patients undergoing primary radiotherapy rather than nodal resection to establish baseline tumor extent for comparison with posttreatment imaging, and patients with indeterminate nodes seen on CT or MRI. In some institutions, FDG PET may also have a role in the detection of the unknown primary tumors and for assessment of recurrent disease.

Trap—Small or cystic nodes can be false-negative on FDG PET.

Trap—FDG uptake is not expected in well-differentiated thyroid carcinoma, although dedifferentiated tumors are typically FDG-avid.

Trap—FDG uptake is variable for medullary thyroid carcinoma, and even large metastases can be FDG-negative [22].

DWI is a simple sequence to include on routine neck MRI. Like the DWI appearances of other malignancies, metastatic cervical lymph nodes have relatively lower apparent diffusion coefficient values when compared with benign lymph nodes [23, 24]. Current research directions are looking at the validity of advanced imaging techniques not just for evaluating nodes for potential malignancy but also for better understanding tumor biology and predicting those tumors likely to respond to chemoradiation [25, 26].

Conclusion

A systematic approach to evaluating lymph nodes is required for head and neck cancer. The four key steps are to systematically search for abnormal nodes, particularly in expected drainage sites; describe location and review check locations; report features important for staging; and evaluate features important for management.

References

1. Kao J, Lavaf A, Teng MS, Huang D, Genden EM. Adjuvant radiotherapy and survival for patients with node-positive head and neck cancer: an analysis by primary site and nodal stage. *Int J Radiat Oncol Biol Phys* 2008; 71:362–370
2. Castelijns JA, van den Brekel MW. Imaging of lymphadenopathy in the neck. *Eur Radiol* 2002; 12:727–738
3. Curtin HD, Ishwaran H, Mancuso AA, Dalley RW, Caudry DJ, McNeil BJ. Comparison of CT and MR imaging in staging of neck metastases. *Radiology* 1998; 207:123–130
4. Schwartz LH, Bogaerts J, Ford R, et al. Evaluation of lymph nodes with RECIST 1.1. *Eur J Cancer* 2009; 45:261–267
5. Kaji AV, Mohuchy T, Swartz JD. Imaging of cervical lymphadenopathy. *Semin Ultrasound CT MR* 1997; 18:220–249

6. Goldenberg D, Begum S, Westra WH, et al. Cystic lymph node metastasis in patients with head and neck cancer: an HPV-associated phenomenon. *Head Neck* 2008; 30:898–903
7. Hudgins PA, Gillison M. Second branchial cleft cyst: not!! (editorial) *AJNR* 2009; 30:1628–1629
8. Eisenkraft BL, Som PM. The spectrum of benign and malignant etiologies of cervical node calcification. *AJR* 1999; 172:1433–1437
9. Som PM. Detection of metastasis in cervical lymph nodes: CT and MR criteria and differential diagnosis. *AJR* 1992; 158:961–969
10. Robbins KT, Clayman G, Levine PA, et al. Neck dissection classification update: revisions proposed by the American Head and Neck Society and the American Academy of Otolaryngology-Head and Neck Surgery. *Arch Otolaryngol Head Neck Surg* 2002; 128:751–758
11. Som PM, Curtin HD, Mancuso AA. Imaging-based nodal classification for evaluation of neck metastatic adenopathy. *AJR* 2000; 174:837–844
12. Nieder C, Gregoire V, Ang KK. Cervical lymph node metastases from occult squamous cell carcinoma: cut down a tree to get an apple? *Int J Radiat Oncol Biol Phys* 2001; 50:727–733
13. Hoang JK, Glastonbury CM, Chen LF, Salvatore JK, Eastwood JD. CT mucosal window settings: a novel approach to evaluating early T-stage head and neck carcinoma. *AJR* 2010; 195:1002–1006
14. Edge SB, American Joint Committee on Cancer. *AJCC cancer staging manual*, 7th ed. New York, NY: Springer-Verlag, 2010:xiv, 648
15. Puri SK, Fan CY, Hanna E. Significance of extracapsular lymph node metastases in patients with head and neck squamous cell carcinoma. *Curr Opin Otolaryngol Head Neck Surg* 2003; 11:119–123
16. Gor DM, Langer JE, Loevner LA. Imaging of cervical lymph nodes in head and neck cancer: the basics. *Radiol Clin North Am* 2006; 44:101–110 [viii]
17. Yu Q, Wang P, Shi H, Luo J. Carotid artery and jugular vein invasion of oral-maxillofacial and neck malignant tumors: diagnostic value of computed tomography. *Oral Surg Oral Med Oral Pathol Oral Radiol Endod* 2003; 96:368–372
18. Yousem DM, Hatabu H, Hurst RW, et al. Carotid artery invasion by head and neck masses: prediction with MR imaging. *Radiology* 1995; 195:715–720
19. Yoo GH, Hocwald E, Korkmaz H, et al. Assessment of carotid artery invasion in patients with head and neck cancer. *Laryngoscope* 2000; 110:386–390
20. King AD, Ahuja AT, Yeung DK, et al. Malignant cervical lymphadenopathy: diagnostic accuracy of diffusion-weighted MR imaging. *Radiology* 2007; 245:806–813
21. Kyzas PA, Evangelou E, Denaxa-Kyza D, Ioannidis JP. ^{18}F-fluorodeoxyglucose positron emission tomography to evaluate cervical node metastases in patients with head and neck squamous cell carcinoma: a meta-analysis. *J Natl Cancer Inst* 2008; 100:712–720
22. Ong SC, Schoder H, Patel SG, et al. Diagnostic accuracy of ^{18}F-FDG PET in restaging patients with medullary thyroid carcinoma and elevated calcitonin levels. *J Nucl Med* 2007; 48:501–507
23. Abdel Razek AA, Soliman NY, Elkhamary S, Alsharaway MK, Tawfik A. Role of diffusion-weighted MR imaging in cervical lymphadenopathy. *Eur Radiol* 2006; 16:1468–1477
24. Vandecaveye V, De Keyzer F, Vander Poorten V, et al. Head and neck squamous cell carcinoma: value of diffusion-weighted MR imaging for nodal staging. *Radiology* 2009; 251:134–146
25. Chawla S, Kim S, Loevner LA, et al. Prediction of disease-free survival in patients with squamous cell carcinomas of the head and neck using dynamic contrast-enhanced MR imaging. *AJNR* 2011; 32:778–784
26. Kim S, Loevner LA, Quon H, et al. Prediction of response to chemoradiation therapy in squamous cell carcinomas of the head and neck using dynamic contrast-enhanced MR imaging. *AJNR* 2010; 31:262–268

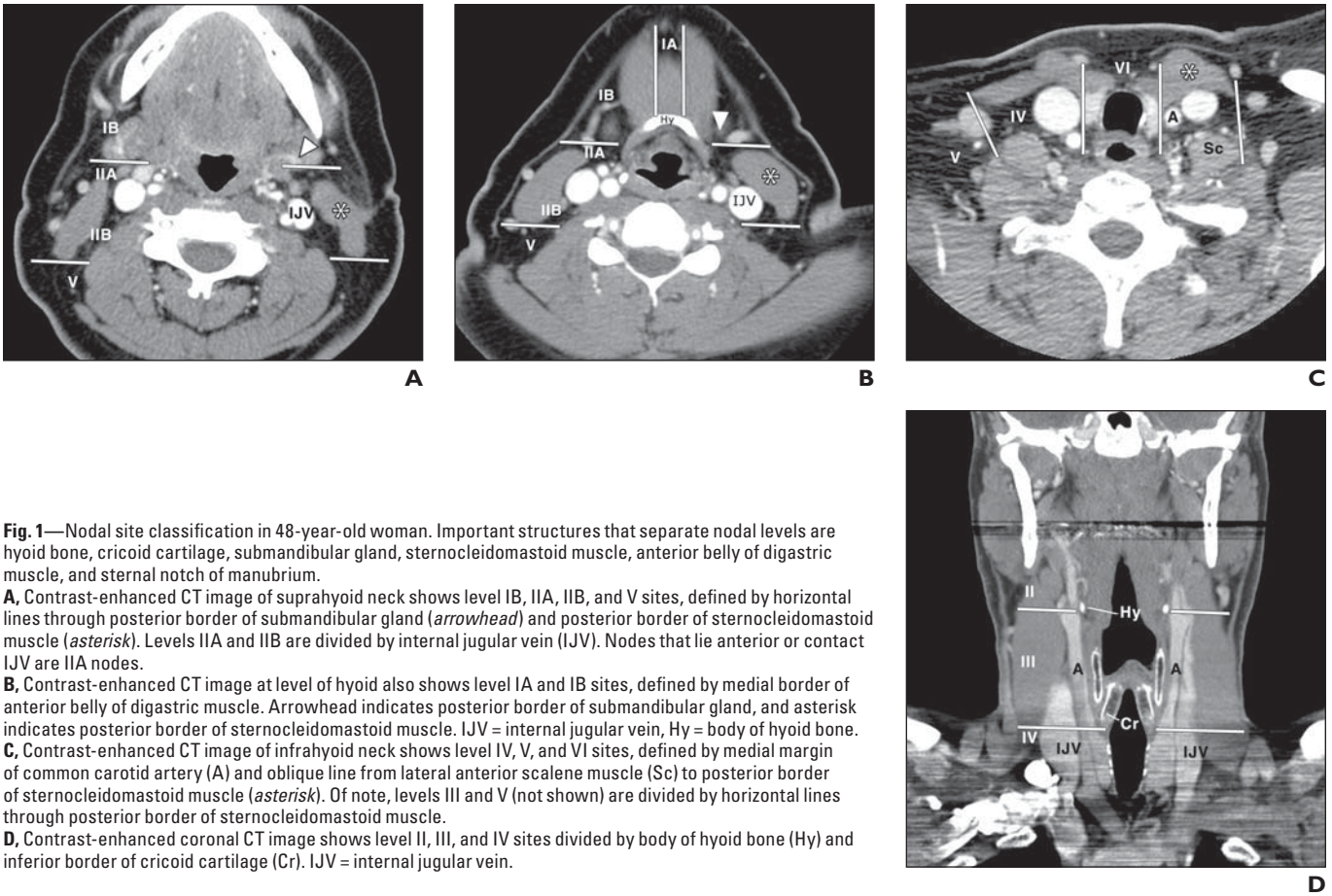

Fig. 1—Nodal site classification in 48-year-old woman. Important structures that separate nodal levels are hyoid bone, cricoid cartilage, submandibular gland, sternocleidomastoid muscle, anterior belly of digastric muscle, and sternal notch of manubrium.

A, Contrast-enhanced CT image of suprahyoid neck shows level IB, IIA, IIB, and V sites, defined by horizontal lines through posterior border of submandibular gland (*arrowhead*) and posterior border of sternocleidomastoid muscle (*asterisk*). Levels IIA and IIB are divided by internal jugular vein (IJV). Nodes that lie anterior or contact IJV are IIA nodes.

B, Contrast-enhanced CT image at level of hyoid also shows level IA and IB sites, defined by medial border of anterior belly of digastric muscle. Arrowhead indicates posterior border of submandibular gland, and asterisk indicates posterior border of sternocleidomastoid muscle. IJV = internal jugular vein, Hy = body of hyoid bone.

C, Contrast-enhanced CT image of infrahyoid neck shows level IV, V, and VI sites, defined by medial margin of common carotid artery (A) and oblique line from lateral anterior scalene muscle (Sc) to posterior border of sternocleidomastoid muscle (*asterisk*). Of note, levels III and V (not shown) are divided by horizontal lines through posterior border of sternocleidomastoid muscle.

D, Contrast-enhanced coronal CT image shows level II, III, and IV sites divided by body of hyoid bone (Hy) and inferior border of cricoid cartilage (Cr). IJV = internal jugular vein.

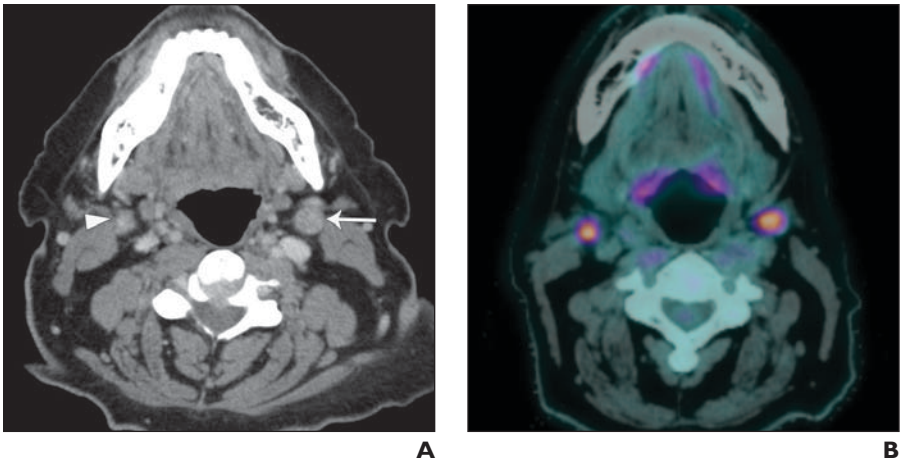

Fig. 2—63-year-old man with soft palate squamous cell carcinoma and clinical N0 neck.
A, Axial CT image shows enlarged rounded left level IIA node (*arrow*) measuring 1.3 cm in axial plane. Because midline tumors can drain bilaterally, contralateral neck should be reviewed with attention. There is also small right level IIA node that has rounded shape and irregular margins suggesting extracapsular spread (*arrowhead*). Although it measured only 8 mm in diameter, these features are very concerning.
B, Axial fused PET/CT image shows that both level IIA nodes have increased ^{18}F-FDG uptake. Detecting bilateral nodal disease changed N stage from N1 (single and < 3 cm) to N2c disease. FDG PET is most commonly performed functional imaging modality and has higher sensitivity and specificity for metastatic nodal disease compared with CT and MRI alone.

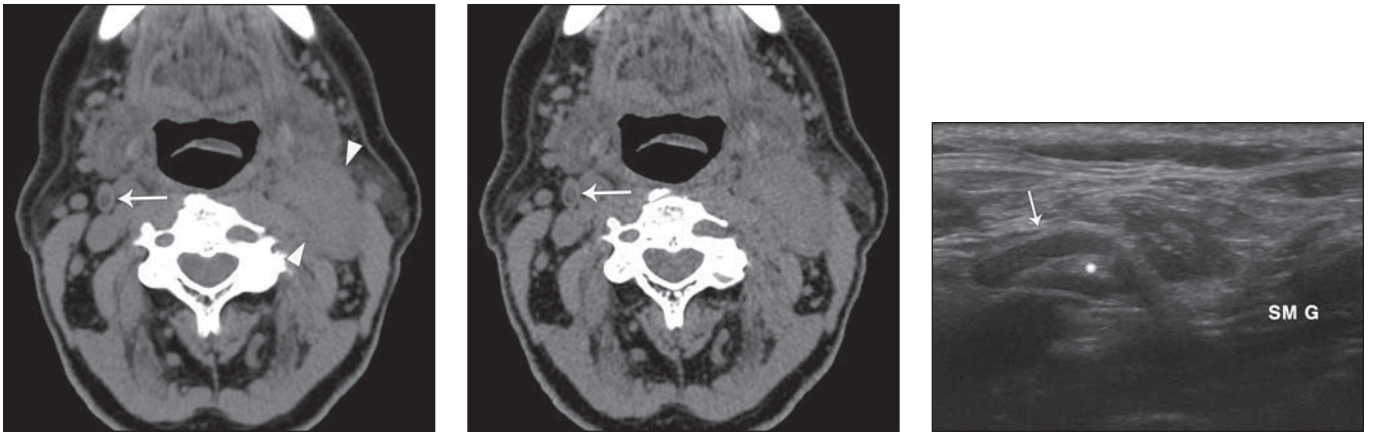

Fig. 3—75-year-old man with invasive squamous cell carcinoma of left tonsil and mimic of necrotic metastasis. CT was performed for nodal staging.
A, Axial unenhanced CT image with slice thickness of 3 mm shows large conglomerate left level IIA nodal mass (*arrowheads*). Prior CT reported subcentimeter necrotic right level IIA node (*arrow*).
B, Axial unenhanced CT image at same level reformatted to 0.6-mm thickness shows that node (*arrow*) is not necrotic but has fatty hilum with central density, representing feeding vessel.
C, Ultrasound image shows normal appearing lymph node (*arrow*) with bean-shape and central echogenic fatty hilum (*asterisk*). Ultrasound is excellent problem-solving tool for equivocal nodes when there might be significant alteration in treatment and allows fine-needle aspiration guidance for these small nodes. SM G = submandibular gland

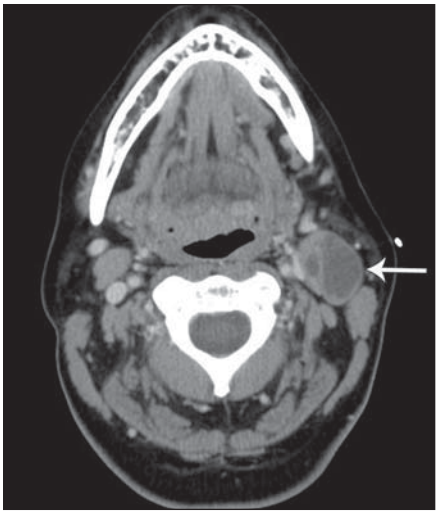

Fig. 4—37-year-old woman with human papilloma virus (HPV)-associated squamous cell carcinoma (SCC) and necrotic nodal metastasis. Patient presented with slowly growing left neck mass that was initially interpreted as infected branchial cleft cyst. Axial contrast-enhanced CT image shows left level IIA necrotic and cystic node (*arrow*) that compresses internal jugular vein. After resection of cystic mass, pathology revealed SCC. Further evaluation of pathologic specimen determined that it was *p16*-positive, representing HPV-associated SCC. Primary tumor was found to be at left base of tongue. HPV-associated SCC can occur in young patients who are nonsmokers and nondrinkers.

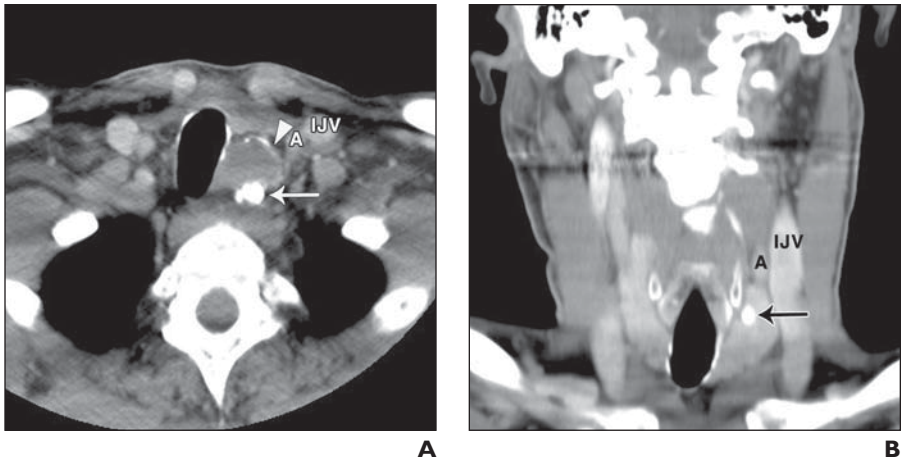

Fig. 5—64-year-old man with papillary thyroid carcinoma and cystic and calcified nodal metastasis. Chest CT was initially performed for staging of neuroendocrine tumor of pancreas. Incidental findings in lower neck led to dedicated neck CT study. A = common carotid artery, IJV = internal jugular vein.
A, Axial contrast-enhanced CT image shows left level VI lymph node with both calcifications (*arrow*) and cystic (*arrowhead*) component. Cyst has thin calcified wall.
B, Coronal contrast-enhanced CT image shows coarsely calcified nodule in left lobe of thyroid (*arrow*). Fine-needle aspiration was performed of both masses and cytology showed papillary thyroid carcinoma. Calcification and cystic change are most often seen with papillary thyroid carcinoma nodal metastases.

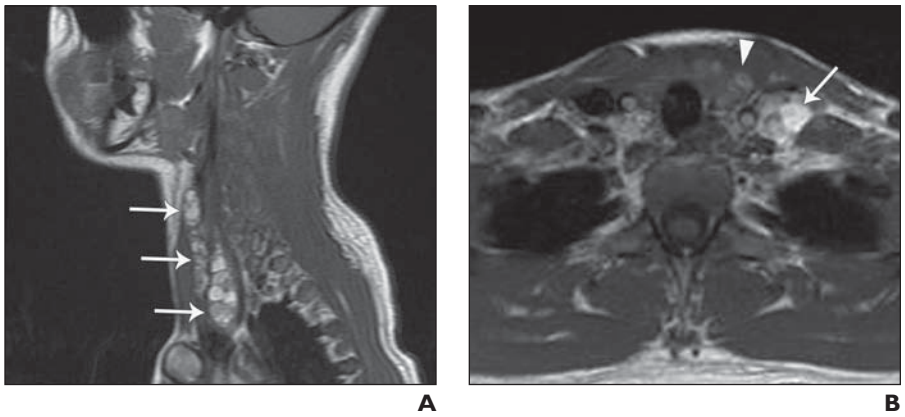

Fig. 6—24-year-old woman with papillary thyroid carcinoma and nodal metastases that are intrinsically hyperintense on T1-weighted imaging. This medical student presented with several-month history of hoarseness for which she had been treated elsewhere with thyroplasty for left vocal cord paralysis.
A, Sagittal unenhanced T1-weighted MR image shows string of small heterogeneous but predominantly hyperintense nodules along left jugular chain (levels III and IV) (*arrows*).
B, Axial unenhanced T1-weighted MR image shows left nodal conglomerate at level IV (*arrow*), lateral to common carotid artery, again showing hyperintensity of these nodes. Notice also heterogeneous appearance of left thyroid lobe (*arrowhead*). Ultrasound-guided fine-needle aspiration found papillary thyroid carcinoma.

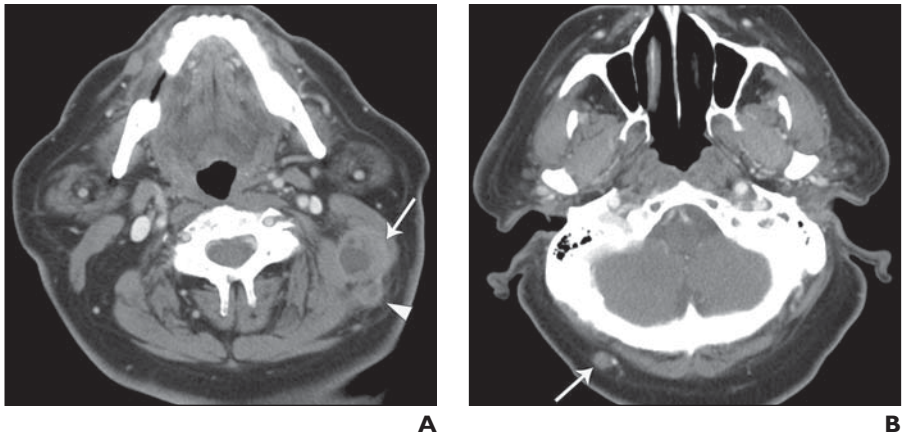

Fig. 7—73-year-old man with skin squamous cell carcinoma of scalp vertex with extracapsular spread of nodal metastases. CT was performed for nodal staging.
A, Axial contrast-enhanced CT image shows enlarged left level IIB (*arrow*) and V (*arrowhead*) nodes that have focal necrosis as well as irregular margins and fat stranding, suggestive of extracapsular spread. Extracapsular spread was confirmed pathologically after neck dissection.
B, Axial contrast-enhanced CT image shows right occipital node (*arrow*) that also proved to be nodal metastasis. Scalp primary tumors have high tendency for bilateral drainage to occipital, intraparotid and facial nodes as well as level V. Although this occipital node was < 1 cm, it is large for this location and is expected drainage site.

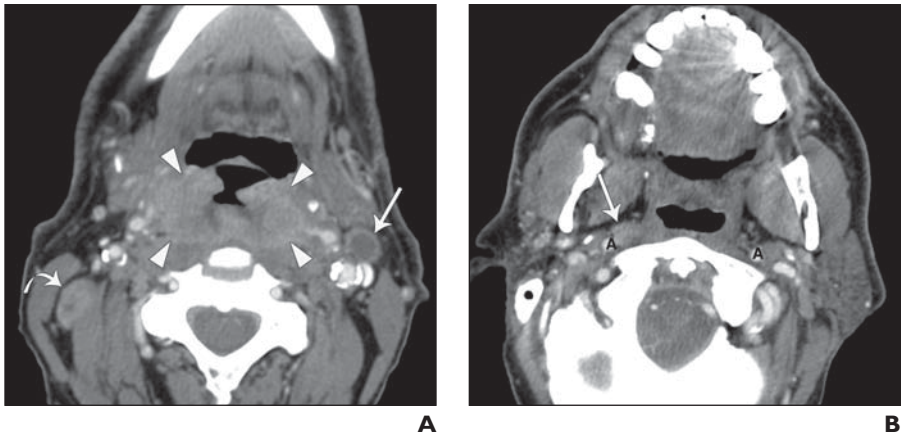

Fig. 8—58-year-old man with squamous cell carcinoma (SCC) of posterior wall of hypopharynx and oropharynx with subtle retropharyngeal nodal metastasis. He presented with progressive weight loss and difficulty swallowing.
A, Axial contrast-enhanced CT image shows irregularly enhancing mass along posterior wall of oropharynx (*arrowheads*). Tumor also extends to posterior wall of hypopharynx. There is cystic left level IIA node (*straight arrow*) and necrotic right level IIB node (*curved arrow*).
B, Axial contrast-enhanced CT image shows small right retropharyngeal node (*arrow*). Note location medial to internal carotid artery (A). SCC of pharynx is more likely to metastasize to retropharyngeal nodes when there is posterior pharyngeal wall involvement.

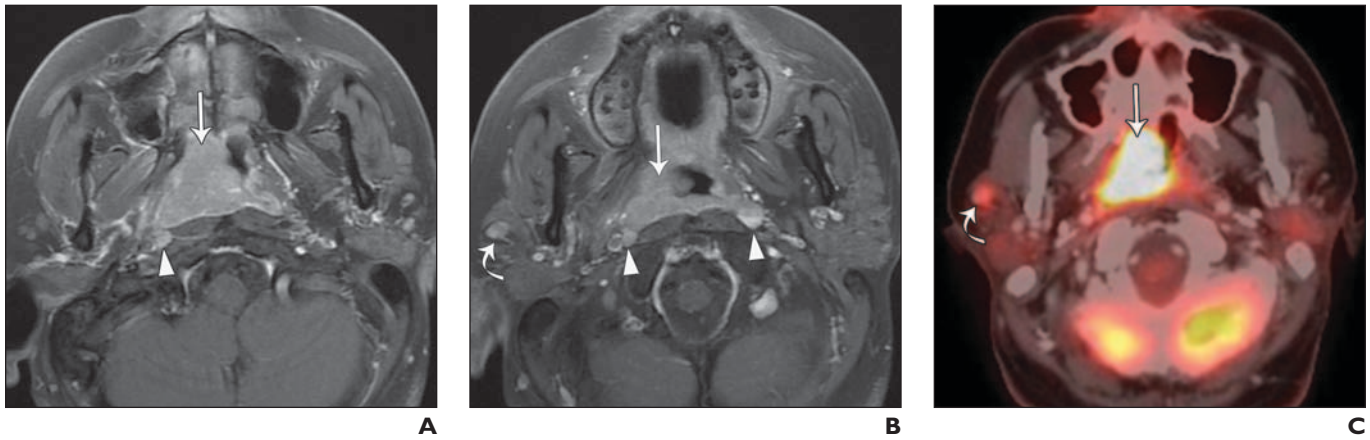

Fig. 9—22-year-old man who presented with nasopharyngeal mass determined to be nasopharyngeal carcinoma.
A and **B,** Axial contrast-enhanced T1-weighted MR images show enhancing right nasopharyngeal mass (*straight arrows*). Enlarged retropharyngeal nodes were evident and proved to be ^{18}F-FDG avid (*arrowheads*). Note rounded right parotid lymph node (*curved arrow*, **B**) without fatty hilum. This parotid node is suspicious because it is potential drainage site for nasopharyngeal carcinoma.
C, Fused axial PET/CT image shows avid uptake in primary tumor (*straight arrow*) as well as in right parotid node (standardized uptake value = 4) (*curved arrow*). Parotid glands are also important potential drainage site for skin neoplasms, including external auditory canal, nasopharynx, and orbit.

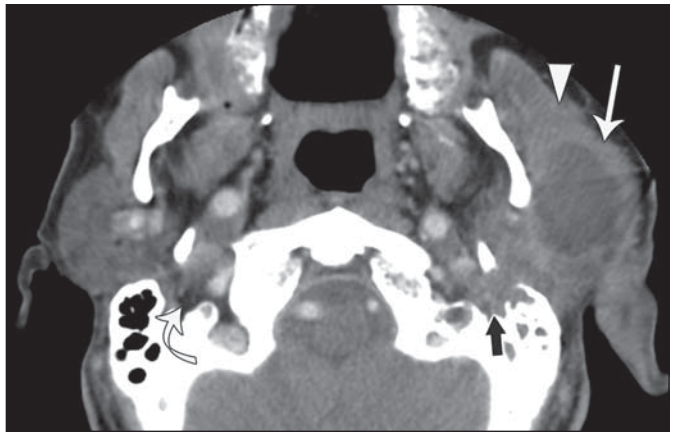

Fig. 10—68-year-old man with perineural and bone invasion from parotid node metastasis. Patient had history of skin squamous cell carcinoma (SCC) of left cheek and presented with left preauricular swelling. Axial contrast-enhanced CT image shows large necrotic left intraparotid lymph node (*straight white arrow*). There is loss of fat plane delineation from masseter muscle suggesting extracapsular spread and muscle invasion (*arrowhead*). There is also soft-tissue density at stylomastoid foramen with associated osseous erosion (*black arrow*). This is highly suggestive of perineural tumor spread from nodal metastasis along facial nerve. Contralateral stylomastoid foramen contains normal fat (*curved arrow*). Biopsy confirmed SCC metastasis within left parotid gland.

Fig. 11—48-year-old woman with vascular invasion from squamous cell carcinoma (SCC) nodal metastasis. Patient was initially treated for right tongue SCC with partial glossectomy and right level I–III neck dissection. All nodes were negative on pathology. Five months after surgery, patient presented with right neck mass that was positive for SCC at biopsy. Axial contrast-enhanced CT image shows right level IIA node with necrosis (*asterisk*), extracapsular spread, and encasement of common carotid artery of 360° (*arrow*). There is also invasion of adjacent sternocleidomastoid muscle (*arrowhead*). A = common carotid artery, IJV = internal jugular vein.

FOR YOUR INFORMATION

This article is available for CME/SAM credit. Log onto www.arrs.org; click on *AJR* (in the blue Publications box); click on the article name; add the article to the cart; proceed through the checkout process.